NEOPLASMA accepted, ahead of print manuscript
Cite article as https://doi.org/10.4149/neo_2026_251204N508

**Running title:** ISO's effects on Huh-7 cells

# Isoguanosine exerts anticancer effects in Huh-7 cells by modulating ROS-dependent MAPK and AKT signaling

An-Qi Wang[1,#], Xiao-Yu Jin[2,#], Ying-Hua Luo[3,#], Nan Wu[1,4,5], Yan-Jun Tang[4,5], Yan-Zhi Liu[1,4,5], Tian-Zhu Li[6,*], Cheng-Hao Jin[1,4,5,*]

[1]Department of Biochemistry and Molecular Biology, College of Life Science and Biotechnology, Heilongjiang Bayi Agricultural University, Daqing, China; [2]Department of CT, Daqing Oilfield General Hospital, Daqing, China; [3]Department of Grass Science, College of Animal Science and Veterinary Medicine, Heilongjiang Bayi Agricultural University, Daqing, China; [4]Department of Food Science and Engineering, College of Food Science, Heilongjiang Bayi Agricultural University, Daqing, China; [5]National Coarse Cereals Engineering Research Center, Daqing, China; [6] Department of Molecular Biology, College of Basic Medical Science, Chifeng University, Chifeng, Inner Mongolia Autonomous Region, China

[*]Correspondence: jinchenghao3727@byau.edu.cn; litianzhu@cfxy.edu.cn

[#]Contributed equally to this work.

**Received December 4, 2025 / Accepted April 9, 2026**

Isoguanosine (ISO) is a naturally occurring bioactive compound with multiple pharmacological properties. In this study, the inhibitory effects of ISO on hepatocellular carcinoma (HCC) cells and its underlying molecular mechanisms were investigated. The cell viability after ISO treatment was assessed using the CCK-8 assay, trypan blue staining, and Hoechst 33342/PI double staining. The relevant targets of ISO and their regulatory mechanisms were predicted using network pharmacology and molecular docking technology. The induction of apoptosis by ISO on Huh-7 cells was detected by Annexin V-FITC/PI double staining combined with flow cytometry and western blotting. The cell cycle arrest effect of ISO on Huh-7 cells was detected by Ki-67 staining, flow cytometry, and western blotting. The migration-inhibition effect of ISO on Huh-7 cells was detected by the wound healing, Transwell, and western blotting. In addition, the effects of reactive oxygen species (ROS) and protein kinase B (AKT) on Huh-7 cells were investigated by using N-acetyl cysteine (NAC) and AKT inhibitor HY10249, respectively. Cell viability assays demonstrated that ISO exerts a significant cytotoxic effect on HCC cell lines. Network pharmacology analysis revealed that the core targets of ISO are associated with ROS, AKT, and mitogen-activated protein kinase (MAPK) signaling pathways. Molecular docking results indicate that ISO has a strong binding affinity for AKT1, CASP3, and GSK3B. Apoptosis assays indicated that ISO induces apoptosis in Huh-7 cells via the mitochondria-dependent pathway. Furthermore, ISO modulates apoptosis through the MAPK and signal transducer and activator of transcription 3 (STAT3) signaling pathways. Cell cycle assays showed that ISO induces G2/M phase arrest by

elevating intracellular ROS levels. Migration assays demonstrated that ISO inhibits cell migration by regulating the AKT signaling pathway. In addition, pretreatment with NAC reversed ISO-induced apoptosis, cell cycle arrest, and inhibition of migration. ISO promotes apoptosis, induces cell cycle arrest, and inhibits Huh-7 cell migration. These findings provide a theoretical basis for further pharmacological research and support the potential development and application of ISO as an anticancer agent.

**Key words:** isoguanosine; hepatocellular carcinoma; cell apoptosis; cell cycle; cell migration; ROS

Hepatocellular carcinoma (HCC) is a malignant tumor originating from hepatocytes cells [1], and it is typically diagnosed at an intermediate or advanced stage [2]. In recent years, the global incidence and mortality rates of HCC has continued to rise annually [3], posing a serious threat to public health and human life [4, 5]. Depending on individual clinical circumstances, patients with liver cancer are commonly treated with surgery, chemotherapy, or radiotherapy [1]. Chemotherapy is a well-established modality in oncology [6, 7]. However, its efficacy is significantly compromised due to frequent adverse effects and the growing problem of resistance to chemotherapeutic agents [8, 9]. Therefore, the development of novel and safe antitumor agents for the treatment of HCC is urgently needed.

Naturally derived compounds extracted from traditional Chinese herbal medicines have demonstrated multi-target and multi-pathway therapeutic effects against various cancers [10-12]. In recent years, the anti-inflammatory, antibacterial, and antitumor properties of isoguanosine (ISO) have garnered significant research interest both domestically and internationally [13-15]. However, studies investigating its efficacy against liver cancer and its precise antitumor mechanisms remain limited. Thus, this study aimed to elucidate whether ISO exerts inhibitory effects on the growth of Huh-7 cells and to explore its associated molecular mechanisms.

Numerous studies have demonstrated that natural or synthetic compounds can induce diverse forms of regulated cell death, including cell apoptosis necroptosis, ferroptosis, pyroptosis, and autophagic cell death, contributing to their anticancer activity [16-18]. A comprehensive understanding of these pathways is essential for exploring the full anticancer mechanisms of bioactive compounds. In this study, we focused on elucidating the apoptotic pathway induced by ISO in Huh- 7 cells. Inducing apoptosis in cancer cells is one of the effective and widely used strategies in cancer treatment [19-21]. Apoptosis can be initiated through mitochondrial pathways or via activation of death

receptors [22, 23]. Reactive oxygen species (ROS), the principal by products of oxidative stress, are known to contribute to tumor initiation and progression [24, 25]. When excessively accumulated, ROS can modulate several signaling pathways, most notably the protein kinase B (AKT) and mitogen-activated protein kinase (MAPK) pathways [26]. These pathways play essential roles in various biological processes, including cell adhesion, survival, and migration [27, 28]. ROS are also involved in regulating the activation of signaling pathways such as AKT and the signal transduction and activator of transcription 3 (STAT3), and may cooperate with the MAPK pathway to promote apoptosis [29, 30].

This study aimed to achieve the following research objectives with corresponding expected outcomes: The main research objective is to predict the ISO-related targets and the regulatory effects of ISO on HCC using network pharmacology methods. To achieve this, we first screened multiple HCC cell lines via the CCK-8 assay and selected Huh-7 cells as the in vitro model for subsequent experiments. We verified the binding affinity of ISO to its predicted target proteins and elucidated its anticancer effects (pro-apoptosis, cell cycle regulation, anti-migration) and underlying molecular mechanisms in Huh-7 cells. Thereby providing a systematic in vitro validation experimental basis for ISO as a potential new anti-HCC candidate drug. The expected result is to identify ROS accumulation as the upstream initiating factor for ISO's anti-HCC effect, and ISO exerts a pro-apoptotic effect by activating the ROS-mediated MAPK/STAT3 signaling pathway to regulate downstream apoptotic proteins. By inhibiting the AKT signaling pathway, cell cycle arrest is induced, and the migration of liver cancer cells is inhibited through the GSK-3β/β-catenin signaling pathway. Ultimately, we obtained systematic experimental data on the multi-pathway regulatory mechanism of ISO on HCC cells, which will lay a solid theoretical and experimental foundation for further pharmacological research on ISO as an anti-cancer drug and its potential clinical development and application.

## Materials and methods

**Cell lines and cell culture.** HCC cell lines Huh-7, HepG2, and Hep3B, along with the human normal lung cell line IMR-90, were obtained from the American Type Culture Collection (ATCC, Manassas, VA, USA). The human normal stomach cell line GES-1, normal liver cell line THLE-2, and normal renal cell line 293T were obtained from Sage Biotechnology Co., Ltd. (Shanghai,

China). All cell lines were cultured in Dulbecco's Modified Eagle's Medium (DMEM; Gibco, Waltham, MA, USA), supplemented with 10% fetal bovine serum (FBS; Gibco), 100 U/ml penicillin, and 100 μg/ml streptomycin (P/S; Gibco). Cells were incubated at 37 °C in a humidified atmosphere containing 5% $CO_2$ in a sterile cell incubator (SanYo, Osaka, Japan). The core experimental model in this study is a hepatocellular carcinoma cell line. The inclusion of normal cell lines was done for the purpose of conducting specific cytotoxicity comparison assessments. All cell lines were obtained from ATCC and tested negative for mycoplasma contamination.

**Cell viability analysis.** Cell viability was assessed using the Cell Counting Kit-8 (CCK-8; Solarbio, Beijing, China), 0.4% Trypan Blue Stain Solution (Coolaber, Beijing, China), and Hoechst 33342/PI Double Staining Kit (Solarbio). To minimize well-to-well variation and edge effects, cells were seeded in equal numbers under consistent experimental conditions. For the CCK-8 assay, cells were seeded into 96-well plates at a density of $1 \times 10^4$ cells/well and treated with various concentrations (20, 40, 60, 80, and 100 μM) of ISO (HerbPurify Co., Chengdu, China) or 5-FU (MedChem Express, Princeton, USA) for different durations (6, 12, 18, 24, and 30 hours (h)). After treatment, 10 μl of CCK-8 solution was added to each well, followed by incubation for an additional 3 h. Absorbance was measured at 490 nm using a microplate reader (Tecan, Shanghai, China) to evaluate cell viability in both carcinoma and normal cell lines.

For the Trypan Blue exclusion assay, Huh-7 cells ($1 \times 10^5$ cells/well) were seeded in 6 cm dishes and treated with 43 μM 5-FU or 27 μM ISO ($IC_{50}$ value) for various time intervals (3, 6, 12, and 24 h). Cells were stained with 0.4% Trypan Blue for 3 minutes (min), and morphological changes were observed under a fluorescence microscope (MSHOT, Guangzhou, China).

For the Hoechst 33342/PI double staining assay, cells were cultured and treated identically to the Trypan Blue assay. Cells were then stained with Hoechst 33342 and propidium iodide (PI) for 20 min according to the manufacturer's instructions, and fluorescence intensity was measured.

**Network pharmacology analysis and molecular docking analysis.** Network pharmacology is a bioinformatics-based approach that integrates multiple omics data to predict drug-target interactions and elucidate underlying mechanisms. In this study, we performed an integrated network pharmacology analysis combined with molecular docking validation to systematically investigate the antitumor mechanism of ISO in HCC. The overall workflow is illustrated in Supplementary Figure S1.

Liver cancer-associated target genes were collected via the GeneCards database (https://www.genecards.org/, accessed on 20 July 2024) using the keyword "hepatocellular carcinoma" and filtering for genes with a relevance score above the median value. The standard linear chemical structure of ISO was obtained from the PubChem database (https://pubchem.ncbi.nlm.nih.gov/, accessed on 20 July 2024), and its 2D and 3D structures were downloaded. Potential ISO-related targets were predicted using the Swiss Target Prediction database (http://www.swisstargetprediction.ch/, accessed on 20 July 2024) with a probability score cutoff > 0.7 and supplemented by literature review. Only human entries were retained, and redundant records were merged.

The Venny 2.1.0 tool (https://bioinfogp.cnb.csic.es/tools/venny/, accessed on 20 July 2024) was used to identify overlapping targets between ISO and HCC. The PPI network was constructed with the following parameters: organism "Homo sapiens," a minimum required interaction score of 0.4, and hiding disconnected nodes in the network. Overlapping genes were submitted to the STRING database (Version 11.0; http://www.string-db.org/, accessed on 20 July 2024), and network visualization and refinement were performed using Cytoscape software (version 3.7.2; https://cytoscape.org/, accessed on 20 July 2024). GO enrichment analysis was carried out using the DAVID platform (https://davidbioinformatics.nih.gov/, accessed on 20 July 2024), along with KEGG pathway enrichment analysis. GO and KEGG enrichment analysis were considered significantly enriched at $p < 0.05$. These analyses revealed key signaling pathways potentially involved in the antitumor effects of ISO.

To validate the binding feasibility between ISO and the key targets predicted by the network pharmacology analysis, molecular docking was performed. The core compound ISO was used as the small-molecule ligand, and the core targets from the PPI network were selected as docking receptors. The two-dimensional SDF structure of ISO was downloaded from the PubChem database, and the PDB-format structures of key target proteins were obtained from the RCSB Protein Data Bank (https://www.rcsb.org/, accessed on 20 July 2024). In PyMOL software, water molecules were removed from the target proteins, and ligand preparation was conducted. Using AutoDockTools 1.5.7, the target proteins were hydrogenated, charges were assigned, and atomic rigid structures were determined. Docking grids were generated to define active binding pockets, and molecular docking was performed using the built-in docking tool. Binding affinities were estimated as free

energy of binding (kcal/mol); lower values indicate stronger interactions. The molecular docking results were visualized using PyMOL software.

**Cell apoptosis analysis.** Apoptosis was analyzed using an Annexin V-FITC/PI apoptosis detection kit (4A Biotech, Beijing, China). The cell culture and treatment conditions were consistent with those used in the Hoechst/PI double staining assay. Briefly, 200 μl of 1× binding buffer and 4 μl of Annexin V-FITC were added to each sample. The cells were incubated in the dark at room temperature for 5 min. Following this, 3 μl of PI was added, and the samples were incubated at 4 °C for 20 min. Apoptotic morphological changes and staining were observed by fluorescence microscopy. In addition, the percentage of apoptotic cells was quantified using flow cytometry (Sysmex Co., Kobe, Japan).

**Mitochondrial membrane potential analysis.** MMP was assessed using the JC-1 MMP assay kit (Solarbio). Huh-7 cells ($1 \times 10^5$ cells/well) were seeded in 6 cm culture dishes and treated with 43 μM 5-FU or 27 μM ISO at various time points (3, 6, 12, and 24 h). After treatment, 1 ml of 1× JC-1 staining solution was added to each well, followed by a 30 min incubation. Cells were then centrifuged for 3 min, washed twice with 1× washing buffer, and subjected to flow cytometry for MMP analysis. The effect of ISO on MMP in Huh-7 cells was recorded.

**Western blotting analysis.** Western blotting was conducted to assess protein expression associated with apoptosis and related pathways. Huh-7 cells ($1 \times 10^5$ cells/well) were cultured in 6 cm dishes and treated with 27 μM ISO for 3, 6, 12, or 24 h. A total of 2 ml of lysis buffer was added to each sample based on cell density. Distilled deionized water (DDW) and 5× sample buffer was added according to optical density (OD) values. Equal amounts of protein (20 μg/sample) were loaded onto SDS–PAGE gels. After electrophoresis and transfer, membranes were incubated with specific antibodies against phosphorylated ERK (p-ERK, #sc-7383), ERK (#sc-154), phosphorylated JNK (p-JNK, #sc-6254), JNK (#sc-7345), phosphorylated p38 (p-p38, #sc-7973), p38 (#sc-7149), phosphorylated AKT (p-AKT, #sc-7985-R), AKT (#sc-8312), phosphorylated STAT3 (p-STAT3, #sc-8059), STAT3 (#sc-8019), Bad (#sc-8044), Bcl-2 (#sc-7382), cytochrome c (cyto-c, #sc-13156), cleaved-caspase-3 (cle-casp-3, #sc-271028), cleaved-PARP (cle-PARP, #sc-8007), Cyclin B1 (#sc-245), CDK1/2 (#sc-53219), p21 (#sc-397), p27 (#sc-528), phosphorylated GSK-3β (p-GSK-3β, #sc-16740-R), GSK-3β (#sc-7291), β-catenin (#sc-7963), E-cadherin (#sc-8426), and N-cadherin (#sc-59987) and α-tubulin (#sc-69971). All aforementioned antibodies were purchased from Santa

Cruz Biotechnology (Dallas, TX, USA). Secondary antibodies, including horseradish peroxidase (HRP)-conjugated goat anti-rabbit IgG and goat anti-mouse IgG, were obtained from ZSGB-Bio (Beijing, China).

**Cell ROS analysis.** ROS levels were analyzed using an ROS detection kit (Solarbio). Huh-7 cells ($1 \times 10^5$ cells/well) were cultured in 6 cm dishes and treated with 43 μM 5-FU or 27 μM ISO at multiple time points (3, 6, 12, and 24 h). Cells were incubated with 2′,7′-dichlorodihydrofluorescein diacetate (DCFH-DA) in the dark for 30 min. ROS accumulation was subsequently measured by flow cytometry and fluorescence microscopy. For further validation, Huh-7 cells were pretreated with N-acetyl cysteine (NAC) for 30 min prior to ISO treatment, and ROS levels were re-evaluated.

**Cell cycle analysis.** Cell cycle analysis was conducted using the Ki67 Cell Proliferation Assay Kit (Beyotime, Shanghai, China) and the DNA Content Quantitative Assay Kit (Solarbio, Beijing, China). Huh-7 cells ($1 \times 10^5$ cells/well) were seeded onto 6 cm culture plates. Subsequently, these cells were treated with 43 μM 5-FU and 27 μM ISO at multiple predetermined time intervals (3, 6, 12, and 24 h). Cells in each well were fixed with 1 ml of fixative for 5 min, followed by the addition of 1 ml of immunostaining blocking solution. After 10 min, 1 ml of Ki67 rabbit monoclonal antibody was added and the samples were incubated overnight at 4 °C. Following three washes with washing solution, 1 ml of anti-rabbit 488 secondary antibody was added and incubated at room temperature for 1 h. Next, 1 ml of nuclear staining solution (DAPI) was added to each well for 5 min. After an additional three washes, the effects of 5-FU and ISO on cell cycle arrest in Huh-7 cells were visualized using fluorescence microscopy.

The cell culture and treatment procedures for DNA content analysis were consistent with the Ki67/PI double staining method. Cells were subsequently fixed in 70% ethanol and stored at 4 °C overnight. The next day, cells were incubated with 100 μL of RNase A at 37 °C for 30 min. Following this, 400 μl of PI was added, and the samples were incubated in the dark at 4 °C for another 30 min. Flow cytometry was then used to evaluate the effects of 5-FU and ISO on cell cycle arrest in Huh-7 cells. Data were subsequently analyzed using Flow Jo 10.8 software. Prior to ISO treatment, Huh-7 cells were pretreated for 30 min with NAC and the AKT inhibitor HY10249, then reanalyzed.

**Cell migration analysis.** Cell migration was assessed using the wound healing assay. Huh-7 cells ($1 \times 10^5$ cells/well) were seeded onto 6 cm culture plates and treated with 43 μM 5-FU and 27 μM

ISO at multiple predetermined time intervals (3, 6, 12, and 24 h). For the Transwell assay, Huh-7 cells at a density of $1 \times 10^5$/ml were seeded into the upper chamber of a Transwell insert. The lower chamber was filled with medium containing 20% FBS and incubated for 24 h. The cells were then treated with 43 μM 5-FU and 27 μM ISO at various time points (3, 6, 12, and 24 h). After incubation, cells were stained using 0.1% crystal violet. Migrated cells were quantified using the Transwell assay and visualized by fluorescence microscopy.

In additional experiments, Huh-7 cells were pretreated with 10 mM NAC for 30 min, or with both 10 mM NAC and the AKT inhibitor HY10249 for 30 min prior to ISO treatment, and migration was reassessed.

**Statistical analysis.** All experiments were conducted in triplicate, and the results were expressed as mean±standard deviation (SD). $IC_{50}$ values were calculated using GraphPad Prism 10.0. One-way analysis of variance (ANOVA) was performed using SPSS 21.0, and statistical significance was determined using T-tests. Significance thresholds were set as follows: $*p < 0.05$, $**p < 0.01$, and $***p < 0.001$.

## Results

**Cytotoxic effects of ISO.** ISO exhibited a potent cytotoxic effect on three HCC cell lines: Huh-7, HepG2, and Hep3B. The cytotoxicity of ISO displayed both concentration and time-dependent effects on liver cancer cell viability (Figures 1A, 1B). In contrast, the toxicity of ISO toward four normal human cell lines-THLE-2, IMR-90, 293T, and GES-1 was significantly lower than that observed for 5-fluorouracil (5-FU) (Figures 1C, 1D). The half-maximal inhibitory concentration ($IC_{50}$) values for Huh-7, HepG2, and Hep3B cells treated with ISO were 27 μM, 80 μM, and 62 μM, respectively. Compared with 5-FU, an increase in the duration of ISO treatment led to a progressive increase in the number of Trypan blue-stained cells (Figure 1E). Additionally, the proportion of Huh-7 cells with both bright Hoechst 33342 and PI fluorescence was increased with prolonged ISO treatment. (Figure 1F). These findings suggest that ISO exerts superior cytotoxicity against Huh-7 cells compared to 5-FU. Consequently, Huh-7 cells were selected as the target model for subsequent experiments.

**ISO and HCC network pharmacology.** To prepare for the subsequent target prediction, we visualized the chemical structure of ISO (Figure 2A). Using SwissTargetPrediction (probability >

0.7, human), we identified 157 potential targets of ISO. From GeneCards (keyword: "hepatocellular carcinoma"), 2349 HCC-related targets were retrieved based on relevance score ≥ median. Venny analysis revealed 110 overlapping targets (Figure 2B). Protein-protein interaction (PPI) networks were constructed using the STRING database and analyzed using Cytoscape software (Figures 2C, 2D). Gene Ontology (GO) analysis indicated that these overlapping targets were mainly associated with the regulation of apoptosis, cell migration, and protein phosphorylation. Kyoto Encyclopedia of Genes and Genomes (KEGG) pathway analysis showed significant enrichment in cancer-related pathways, particularly those involving AKT, MAPK, and ROS signaling (Figures 2E-2G).

**ISO and HCC molecular docking analysis.** To predict the binding sites through which ISO interacts with liver cancer targets, a molecular docking analysis was performed. A comprehensive binding site map of ISO was generated using AutoDock Tools 1.5.7. AKT1, CASP3, and GSK3B were selected as the core protein receptors for docking simulations. The active docking pocket was set, and ISO formed hydrogen bonds with AKT1, CASP3, and GSK3B, indicating favorable docking conformations. Molecular docking models of ISO bound to AKT1, CASP3, and GSK3B were obtained from the PDB database (Figure 2H). The binding interfaces between ISO and AKT1 or GSK3B included residues such as LEU, which may influence phosphorylation activity. These results suggest that ISO exhibits strong binding affinity toward AKT1, CASP3, and GSK3B.

**ISO induces mitochondria-mediated apoptosis in Huh-7 cells.** With prolonged ISO treatment, Huh-7 cells exhibited gradual shrinkage and nuclear fragmentation, and the proportion of apoptotic cells was increased. These morphological changes were more significant than those in the 5-FU-treated group. (Figure 3A). Flow cytometry analysis revealed that ISO increased the proportion of apoptotic cells from 0.02% to 21.55%, while simultaneously reducing mitochondrial membrane potential (MMP) from 99.48% to 77.8% (Figures 3B, 3C). Western blotting results demonstrated that with prolonged ISO treatment, the expression levels of pro-apoptotic proteins including Bad, cytochrome c (cyto-c), cleaved caspase-3 (cle-casp-3), and cleaved PARP (cle-PARP) progressively increased. In contrast, the anti-apoptotic protein Bcl-2 exhibited reduced expression (Figure 3D). These findings indicate that ISO induces mitochondria-dependent apoptosis in Huh-7 cells.

**ISO regulates MAPK/STAT3 signaling pathways in Huh-7 cells.** With increasing ISO treatment time, the expression levels of phosphorylated JNK (p-JNK) and phosphorylated p38 (p-p38)

increased, while the levels of phosphorylated ERK (p-ERK) and phosphorylated STAT3 (p-STAT3) decreased (Figure 3E). To investigate the interaction between MAPK and STAT3 signaling pathways, MAPK inhibitors were applied to Huh-7 cells. ERK inhibition led to decreased p-STAT3 expression, whereas JNK and p38 inhibitors altered these effects (Figures 3F-3H). These results suggest that the MAPK pathway promotes apoptosis in Huh-7 cells through modulation of the STAT3 signaling pathway.

**ISO upregulates ROS levels via MAPK/STAT3 signaling pathways in Huh-7 cells.** ISO treatment led to a progressive increase in ROS accumulation within Huh-7 cells. Compared with 5-FU, ISO induced a greater increase in ROS fluorescence intensity over time (Figures 4A-4C). In the ISO+NAC group, fluorescence intensity was considerably reduced relative to ISO treatment alone, indicating effective ROS scavenging by NAC. Pretreatment with NAC for 30 min significantly reduced the number of apoptotic Huh-7 cells (Figure 4D). Furthermore, the expression levels of p-ERK, p-JNK, p-p38, p-STAT3, cle-casp-3, and cle-PARP were inhibited in the ISO+NAC group compared with ISO treatment alone (Figure 4E). These results collectively demonstrate that ISO elevates intracellular ROS levels, which in turn mediate apoptosis through the MAPK signaling pathway in Huh-7 cells.

**ISO Triggers G2/M cell cycle arrest in Huh-7 cells.** As ISO treatment duration increased, the fluorescence intensity of Huh-7 cells stained with Ki67 decreased, indicating suppressed proliferation. The effect was comparable to that of 5-FU (Figure 5A). Flow cytometry results showed that ISO treatment significantly elevated the proportion of Huh-7 cells in the G2/M phase from 11.7% to 34.9%, while the percentage of cells in the G0/G1 phase progressively declined (Figure 5B). When comparing the ISO+NAC group with ISO treatment alone, the ISO-induced G2/M phase arrest increased from 16.8% to 27.3% (Figure 5C). Western blotting analysis revealed that ISO significantly downregulated the expression of p-AKT, CDK1/2, and Cyclin B, while upregulating p21 and p27 levels in Huh-7 cells. Following pretreatment with NAC or the AKT inhibitor HY10249, marked changes in cell cycle-related protein expression were also observed relative to the inhibitor-only groups (Figures 5C, 5D). These findings demonstrate that ISO can induce G2/M phase cell cycle arrest in Huh-7 cells.

**ISO prevents Huh-7 cell migration via the AKT/GSK-3β/β-catenin signaling pathways.** Inverted fluorescence microscopy revealed that ISO significantly inhibited Huh-7 cell migration

compared with 5-FU, with a time-dependent effect (Figures 6A-6D). Western blotting demonstrated increased expression of E-cadherin and reduced expression of p-AKT, p-GSK-3β, N-cadherin, and β-catenin following ISO treatment. The addition of NAC or the AKT inhibitor HY10249 suppressed these protein expression changes (Figures 6E-6G). Collectively, these findings indicate that ISO impairs Huh-7 cell migration by regulating the AKT/GSK-3β/β-catenin signaling pathways.

## Discussion

In recent years, the use of Chinese herbal medicine in tumor therapy has gained increasing attention due to its potential to inhibit tumor growth and induce apoptosis in cancer cells [31-34]. Croton, a traditional Chinese herb, has demonstrated therapeutic properties including antibacterial, anti-inflammatory, and antiproliferative effects, particularly in MDA-MB-231 breast cancer cells [35]. ISO, the focus of this study, is an important alkaloid component derived from croton [36]. However, the precise molecular mechanisms underlying ISO's anticancer activity have not yet been fully elucidated. 5-FU is a widely used chemotherapeutic agent known to induce apoptosis in various cancer types [37]. Our results demonstrated that ISO significantly inhibited Huh-7 cell proliferation while exerting lower cytotoxicity on normal cells compared with 5-FU, suggesting that ISO may represent a more promising candidate for anticancer drug development. Notably, ISO was shown to induce G2/M cell cycle arrest, apoptosis, and inhibition of migration, primarily through the upregulation of intracellular ROS.

Apoptosis is a tightly regulated process triggered in response to external environmental stressors and involves complex molecular pathways [38, 39]. Members of the Bcl-2 protein family play a pivotal role in modulating mitochondrial membrane permeability [40, 41]. A decrease in MMP facilitates cyto-c release, activates caspase-3, and ultimately leads to programmed cell death [42-44]. Previous studies on croton extracts have shown that they can activate caspase cascades and modulate pro- and anti-apoptotic gene expression to induce mitochondrial-mediated apoptosis [35]. Consistent with these findings, our study demonstrated that ISO increased the expression of the pro-apoptotic protein Bad, decreased Bcl-2 expression, reduced MMP, and triggered apoptosis in Huh-7 cells.

To further elucidate the mechanisms underlying ISO-induced apoptosis, we employed network pharmacology. The analysis revealed enhanced protein phosphorylation activity, with protein kinase and serine/threonine/tyrosine kinase functions playing central roles in the biological processes. MAPK, a serine/threonine kinase, is critically involved in cancer cell apoptosis initiated by natural compounds [45, 46]. In our study, ISO significantly downregulated the expression levels of p-ERK and p-STAT3, further implicating these pathways in its pro-apoptotic effects.

ROS are key regulators of tumor biology, influencing tumor progression, signaling, and cell death [47]. Croton-derived compounds have previously been shown to elevate ROS levels in breast cancer

cells [35]. Consistent with this, our findings demonstrated that ISO induced a sustained increase in ROS levels in Huh-7 cells. To assess the role of ROS in ISO-induced apoptosis, NAC (a ROS scavenger) was used for pretreatment. NAC significantly reduced the proportion of apoptotic cells and altered the expression of key proteins in the AKT, MAPK, and STAT3 pathways. These observations suggest that ROS serve as upstream signals in ISO-induced activation of these pathways, promoting apoptosis through enhanced mitochondrial ROS production. Collectively, these findings indicate that ISO is a promising candidate for development as a novel antitumor agent.

Cell cycle regulation plays a fundamental role in controlling cell proliferation and apoptosis, and is critically involved in tumor initiation and progression [48]. Due to significant variability across cell cycle phases, precise control of cell cycle dynamics remains challenging [49]. Recent studies have shown that various anticancer agents can induce cell cycle arrest and stabilize cell cycle checkpoints [50, 51]. The natural product B10G5 derived from Croton tiglium has been reported to induce G2/M phase arrest and initiate apoptosis in lung cancer cells [52]. In our study, ISO was found to induce G2/M phase arrest in Huh-7 cells by downregulating AKT expression, leading to decreased levels of p-AKT, CDK1/2, and Cyclin B1, and increased levels of p27 and p21. These changes effectively contributed to the suppression of tumorigenic potential.

Cell migration is essential for maintaining tissue organization [53]. β-catenin is a well-known substrate of GSK-3β, and its phosphorylation is modulated by GSK-3β activity [54]. Overexpression or activation of GSK-3β can promote AKT phosphorylation, which is implicated in tumor progression and cell motility [55]. Our results showed that ISO decreased the expression of N-cadherin, increased E-cadherin levels, and inhibited Huh-7 cell migration. Moreover, NAC pretreatment abrogated these effects by suppressing ROS accumulation and its downstream influence on migration-associated proteins. These findings suggest that ISO impairs Huh-7 cell migration through ROS-induced modulation of the AKT/GSK-3β/β-catenin signaling pathway.

The strength of this study lies in the integration of network pharmacology, molecular docking, and experimental validation to systematically elucidate the antitumor mechanism of ISO in HCC. This multidisciplinary approach not only identified key signaling pathways (e.g., AKT, MAPK, STAT3) but also linked them to functional phenotypes such as apoptosis, cell cycle arrest, and migration inhibition, providing a comprehensive mechanistic framework. The convergence of computational

prediction and in vitro validation enhances the reliability and translational potential of the findings. However, this study has certain limitations that should be acknowledged. The absence of in vivo animal model data limits the translation of our cellular findings to a whole-organism context. Future studies employing orthotopic or xenograft mouse models are essential to confirm the antitumor efficacy and safety profile of ISO in vivo. Beyond conventional cytotoxicity, exploring ISO within the context of drug repurposing and sustainable therapeutic strategies could be highly valuable. Specifically, repurposing drugs as GLP-1-based therapies or targeting 20S proteasomes as a prophylactic strategy with immunomodulatory effects has shown positive impacts on cancer management [56, 57]. Future work could investigate whether ISO or its derivatives share mechanistic similarities with these approaches, potentially positioning it within a broader framework for cancer prevention or combination therapy. We believe that addressing these limitations in future research will help fully exploit the potential of ISO as a novel therapeutic agent for HCC.

In summary, ISO induces apoptosis in Huh-7 cells through ROS accumulation, which activates the MAPK/STAT3 signaling pathways and modulates downstream apoptotic proteins. Simultaneously, ISO inhibits the AKT signaling pathway to induce G2/M phase cell cycle arrest and suppresses cell migration via ROS-mediated regulation of the GSK-3β/β-catenin axis. These findings (Figure 7) provide a theoretical basis for further pharmacological research and support the potential development and application of ISO as an anticancer agent.

Acknowledgements: We thank LetPub (www.letpub.com) for their linguistic assistance during the preparation of this manuscript.

This research was funded by, the National Natural Science Foundation of China (Grant No. 82460126), the Program for Young Talents of Science and Technology in Universities of Inner Mongolia Autonomous Region (Grant No. NJYT24032), and the Heilongjiang Province Key Re-search and Development Plan Guidance Project (Grant No. GZ20220039).

**Supplementary data are available in the online version of the paper.**

## References


[1] LLOVET JM, ZUCMAN-ROSSI J, PIKARSKY E, SANGRO B, SCHWARTZ M et al. Hepatocellular carcinoma. Nat Rev Dis Primers 2016; 2: 16018. https://doi.org/10.1038/nrdp.2016.18

[2] FORNER A, REIG M, BRUIX J. Hepatocellular carcinoma. Lancet 2018; 391: 1301-1314. https://doi.org/10.1016/s0140-6736(18)30010-2

[3] FOGLIA B, TURATO C, CANNITO S. Hepatocellular Carcinoma: Latest Research in Pathogenesis, Detection and Treatment. Int J Mol Sci 2023; 24: 12224. https://doi.org/10.3390/ijms241512224

[4] YOUNESS RA, HASSAN HA, ABAZA T, HADY AA, EL MAGDOUB HM et al. A Comprehensive Insight and In Silico Analysis of CircRNAs in Hepatocellular Carcinoma: A Step toward ncRNA-Based Precision Medicine. Cells 2024; 13: 1245. https://doi.org/10.3390/cells13151245

[5] SIM HW, KNOX J. Hepatocellular carcinoma in the era of immunotherapy. Curr Probl Cancer 2018; 42: 40-48. https://doi.org/10.1016/j.currproblcancer.2017.10.007

[6] NYGREN P. What is cancer chemotherapy? Acta Oncol 2001; 40: 166-174. https://doi.org/10.1080/02841860151116204

[7] WIEMANN MC, CALABRESI P. Principles of current cancer chemotherapy. Compr Ther 1983; 9: 46-52.

[8] CHEN LC, LIN HY, HUNG SK, CHIOU WY, LEE MS. Role of modern radiotherapy in managing patients with hepatocellular carcinoma. World J Gastroenterol 2021; 27: 2434-2457. https://doi.org/10.3748/wjg.v27.i20.2434

[9] ORONSKY B, SCICINSKI J, KIM MM, CABRALES P, SALACZ ME et al. Turning on the Radio: Epigenetic Inhibitors as Potential Radiopriming Agents. Biomolecules 2016; 6: 32. https://doi.org/10.3390/biom6030032

[10] WANG C, SHI CH, BAI HY, LU J, HU HT et al. Astragali radix - Curcumae rhizoma herb pair suppresses hepatocellular carcinoma through EGFR/AKT/mTOR pathway and induces lipid peroxidation-related ferroptosis via HIF-1α/HO-1/GPX4 axis. J Ethnopharmacol 2025; 348: 119912. https://doi.org/10.1016/j.jep.2025.119912

[11] ZHONG M, LI Y, WANG H, FAN N, CHU X et al. Integrated network pharmacology and experimental validation reveal EGFR/p53/Bcl-2-mediated anti-hepatocellular carcinoma effects of Zedoary Turmeric Oil. J Ethnopharmacol 2025; 352: 120241. https://doi.org/10.1016/j.jep.2025.120241

[12] ZHAI B, ZHANG N, HAN X, LI Q, ZHANG M et al. Molecular targets of β-elemene, a herbal extract used in traditional Chinese medicine, and its potential role in cancer therapy: A review. Biomed Pharmacother 2019; 114: 108812. https://doi.org/10.1016/j.biopha.2019.108812

[13] DING T, TANG F, NI G, LIU J, ZHAO H et al. The development of isoguanosine: from discovery, synthesis, and modification to supramolecular structures and potential applications. RSC Adv 2020, 10: 6223-6248. https://doi.org/10.1039/C9RA09427J

[14] KIM JH, LEE SJ, HAN YB, MOON JJ, KIM JB. Isolation of isoguanosine from Croton tiglium and its antitumor activity. Arch Pharm Res 1994; 17: 115-118. https://doi.org/10.1007/bf02974234

[15] ZHAO H, FENG H, LIU J, TANG F, DU Y et al. Dual-functional guanosine-based hydrogel integrating localized delivery and anticancer activities for cancer therapy. Biomaterials 2020; 230: 119598. https://doi.org/10.1016/j.biomaterials.2019.119598
[16] YU L, HUANG K, LIAO Y, WANG L, SETHI G et al. Targeting novel regulated cell death: Ferroptosis, pyroptosis and necroptosis in anti-PD-1/PD-L1 cancer immunotherapy. Cell Prolif 2024; 57: e13644. https://doi.org/10.1111/cpr.13644
[17] LI R, WU Y, LI Y, SHUAI W, WANG A et al. Targeted regulated cell death with small molecule compounds in colorectal cancer: Current perspectives of targeted therapy and molecular mechanisms. Eur J Med Chem 2024; 265: 116040. https://doi.org/10.1016/j.ejmech.2023.116040
[18] QIN R, YOU FM, ZHAO Q, XIE X, PENG C et al. Naturally derived indole alkaloids targeting regulated cell death (RCD) for cancer therapy: from molecular mechanisms to potential therapeutic targets. J Hematol Oncol 2022; 15: 133. https://doi.org/10.1186/s13045-022-01350-z
[19] KIM C, KIM B. Anti-Cancer Natural Products and Their Bioactive Compounds Inducing ER Stress-Mediated Apoptosis: A Review. Nutrients 2018; 10: 1021. https://doi.org/10.3390/nu10081021
[20] TONG X, TANG R, XIAO M, XU J, WANG W et al. Targeting cell death pathways for cancer therapy: recent developments in necroptosis, pyroptosis, ferroptosis, and cuproptosis research. J Hematol Oncol 2022; 15: 174. https://doi.org/10.1186/s13045-022-01392-3
[21] XU X, LAI Y, HUA ZC. Apoptosis and apoptotic body: disease message and therapeutic target potentials. Biosci Rep 2019; 39: BSR20180992. https://doi.org/10.1042/bsr20180992
[22] JEONG SY, SEOL DW. The role of mitochondria in apoptosis. BMB Rep 2008; 41: 11-22. https://doi.org/10.5483/bmbrep.2008.41.1.011
[23] WANG H, ZHANG C, LI M, LIU C, WANG J et al. Antimicrobial Peptides Mediate Apoptosis by Changing Mitochondrial Membrane Permeability. Int J Mol Sci 2022; 23: 12732. https://doi.org/10.3390/ijms232112732
[24] SAHOO BM, BANIK BK, BORAH P, JAIN A. Reactive Oxygen Species (ROS): Key Components in Cancer Therapies. Anticancer Agents Med Chem 2022; 22: 215-222. https://doi.org/10.2174/1871520621666210608095512
[25] BRIEGER K, SCHIAVONE S, MILLER FJ JR, KRAUSE KH. Reactive oxygen species: from health to disease. Swiss Med Wkly 2012; 142: w13659. https://doi.org/10.4414/smw.2012.13659
[26] PAN Z, WANG K, WANG X, JIA Z, YANG Y et al. Cholesterol promotes EGFR-TKIs resistance in NSCLC by inducing EGFR/Src/Erk/SP1 signaling-mediated ERRα re-expression. Mol Cancer 2022; 21: 77. https://doi.org/10.1186/s12943-022-01547-3
[27] CHEN Z, OH D, DUBEY AK, YAO M, YANG B et al. EGFR family and Src family kinase interactions: mechanics matters? Curr Opin Cell Biol 2018; 51: 97-102. https://doi.org/10.1016/j.ceb.2017.12.003
[28] TICE DA, BISCARDI JS, NICKLES AL, PARSONS SJ. Mechanism of biological synergy between cellular Src and epidermal growth factor receptor. Proc Natl Acad Sci U S A 1999; 96: 1415-1420. https://doi.org/10.1073/pnas.96.4.1415
[29] BASU A, DAS AS, BORAH PK, DUARY RK, MUKHOPADHYAY R. Biochanin A impedes STAT3 activation by upregulating p38δ MAPK phosphorylation in IL-6-stimulated

macrophages. Inflamm Res 2020; 69: 1143-1156. https://doi.org/10.1007/s00011-020-01387-1

[30] MENG A, ZHANG X, SHI Y. Role of p38 MAPK and STAT3 in lipopolysaccharide-stimulated mouse alveolar macrophages. Exp Ther Med 2014; 8: 1772-1776. https://doi.org/10.3892/etm.2014.2023

[31] DAI XZ, YIN HT, SUN LF, HU X, ZHOU C et al. Potential therapeutic efficacy of curcumin in liver cancer. Asian Pac J Cancer Prev 2013; 14: 3855-3859. https://doi.org/10.7314/apjcp.2013.14.6.3855

[32] LUO H, VONG CT, CHEN H, GAO Y, LYU P et al. Naturally occurring anti-cancer compounds: shining from Chinese herbal medicine. Chin Med 2019; 14: 48. https://doi.org/10.1186/s13020-019-0270-9

[33] YAN Z, LAI Z, LIN J. Anticancer Properties of Traditional Chinese Medicine. Comb Chem High Throughput Screen 2017; 20: 423-429. https://doi.org/10.2174/1386207320666170116141818

[34] ZHANG X, QIU H, LI C, CAI P, QI F. The positive role of traditional Chinese medicine as an adjunctive therapy for cancer. Biosci Trends 2021; 15: 283-298. https://doi.org/10.5582/bst.2021.01318

[35] POOFERY J, SRIPANIDKULCHAI B, BANJERDPONGCHAI R. Extracts of Bridelia ovata and Croton oblongifolius induce apoptosis in human MDA- MB- 231 breast cancer cells via oxidative stress and mitochondrial pathways. Int J Oncol 2020; 56: 969-985. https://doi.org/10.3892/ijo.2020.4973

[36] YAN P, ZHANG L, PENG C, ZHANG R. Pharmacokinetics and tissue distribution of crotonoside. Xenobiotica 2018; 48: 28-36. https://doi.org/10.1080/00498254.2016.1276311

[37] LACOURSE KD, ZEPEDA-RIVERA M, KEMPCHINSKY AG, BARYIAMES A, MINOT SS et al. The cancer chemotherapeutic 5-fluorouracil is a potent Fusobacterium nucleatum inhibitor and its activity is modified by intratumoral microbiota. Cell Rep 2022; 41: 111625. https://doi.org/10.1016/j.celrep.2022.111625

[38] KASHYAP D, GARG VK, GOEL N. Intrinsic and extrinsic pathways of apoptosis: Role in cancer development and prognosis. Adv Protein Chem Struct Biol 2021; 125: 73-120. https://doi.org/10.1016/bs.apcsb.2021.01.003

[39] D'ARCY MS. Cell death: a review of the major forms of apoptosis, necrosis and autophagy. Cell Biol Int 2019; 43: 582-592. https://doi.org/10.1002/cbin.11137

[40] KLUCK RM, BOSSY-WETZEL E, GREEN DR, NEWMEYER DD. The release of cytochrome c from mitochondria: a primary site for Bcl-2 regulation of apoptosis. Science 1997; 275: 1132-1136. https://doi.org/10.1126/science.275.5303.1132

[41] HARRIS MH, THOMPSON CB. The role of the Bcl-2 family in the regulation of outer mitochondrial membrane permeability. Cell Death Differ 2000; 7: 1182-1191. https://doi.org/10.1038/sj.cdd.4400781

[42] CHONG SJ, LOW IC, PERVAIZ S. Mitochondrial ROS and involvement of Bcl-2 as a mitochondrial ROS regulator. Mitochondrion 2014; 19: 39-48. https://doi.org/10.1016/j.mito.2014.06.002

[43] ITO T. [Overexpression of bcl-2 suppresses apoptosis in the human leukemia cell line TF-1] Rinsho Byori 1997; 45: 628-637.

[44] KALONI D, DIEPSTRATEN ST, STRASSER A, KELLY GL. BCL-2 protein family: attractive targets for cancer therapy. Apoptosis 2023; 28: 20-38. https://doi.org/10.1007/s10495-022-01780-7
[45] FANG JY, RICHARDSON BC. The MAPK signalling pathways and colorectal cancer. Lancet Oncol 2005; 6: 322-327. https://doi.org/10.1016/s1470-2045(05)70168-6
[46] ASL ER, AMINI M, NAJAFI S, MANSOORI B, MOKHTARZADEH A et al. Interplay between MAPK/ERK signaling pathway and MicroRNAs: A crucial mechanism regulating cancer cell metabolism and tumor progression. Life Sci 2021; 278: 119499.
[47] MOLONEY JN, COTTER TG. ROS signalling in the biology of cancer. Semin Cell Dev Biol 2018; 80: 50-64. https://doi.org/10.1016/j.semcdb.2017.05.023
[48] SUN Y, LIU Y, MA X, HU H. The Influence of Cell Cycle Regulation on Chemotherapy. Int J Mol Sci 2021; 22. https://doi.org/10.3390/ijms22136923
[49] ONG G, LIU J, TANG X, ZHONG J, ZENG Y et al. Cell cycle checkpoint revolution: targeted therapies in the fight against malignant tumors. Front Pharmacol 2024; 15: 1459057. https://doi.org/10.3389/fphar.2024.1459057
[50] LIU Y, WANG Y, YANG Y, QUAN Y, GUO M. Liquiritigenin Induces Cell Cycle Arrest and Apoptosis in Lung Squamous Cell Carcinoma. Cell Biochem Biophys 2024; 82: 1397-1407. https://doi.org/10.1007/s12013-024-01294-w
[51] LIU J, LI SM, TANG YJ, CAO JL, HOU WS et al. Jaceosidin induces apoptosis and inhibits migration in AGS gastric cancer cells by regulating ROS-mediated signaling pathways. Redox Rep 2024; 29: 2313366. https://doi.org/10.1080/13510002.2024.2313366
[52] WANG Y, TANG C, YAO S, LAI H, LI R et al. Discovery of a novel protein kinase C activator from Croton tiglium for inhibition of non-small cell lung cancer. Phytomedicine 2019; 65: 153100. https://doi.org/10.1016/j.phymed.2019.153100
[53] TREPAT X, CHEN Z, JACOBSON K. Cell migration. Compr Physiol 2012; 2: 2369-2392. https://doi.org/10.1002/cphy.c110012
[54] YOST C, TORRES M, MILLER JR, HUANG E, KIMELMAN D, et al. The axis-inducing activity, stability, and subcellular distribution of beta-catenin is regulated in Xenopus embryos by glycogen synthase kinase 3. Genes Dev 1996; 10: 1443-1454. https://doi.org/10.1101/gad.10.12.1443
[55] WAN G, LIU Y, ZHU J, GUO L, LI C, et al. SLFN5 suppresses cancer cell migration and invasion by inhibiting MT1-MMP expression via AKT/GSK-3β/β-catenin pathway. Cell Signal 2019; 59: 1-12. https://doi.org/10.1016/j.cellsig.2019.03.004
[56] MOSTAFA AM, HAMDY NM, ABDEL-RAHMAN SZ, EL-MESALLAMY HO. Effect of vildagliptin and pravastatin combination on cholesterol efflux in adipocytes. IUBMB Life 2016; 68: 535-543. https://doi.org/10.1002/iub.1510
[57] ATTA H, ALZAHABY N, HAMDY NM, EMAM SH, SONOUSI A, et al. New trends in synthetic drugs and natural products targeting 20S proteasomes in cancers. Bioorg Chem 2023; 133: 106427. https://doi.org/10.1016/j.bioorg.2023.106427

## Figure Legends

**Figure 1.** Cytotoxic effects of isoguanosine (ISO) in hepatocellular carcinoma (HCC) cells. Cell

viability was assessed using the CCK-8 assay. A) Huh-7, HepG2, and Hep3B cells were treated with various concentrations (0, 20, 40, 60, 80, and 100 μM) of ISO and 5-FU for 24 h. B) Cells were treated with 27 μM ISO or 5-FU for 6, 12, 18, 24, and 30 h. C) Normal cell lines (THLE-2, IMR-90, 293T, and GES-1) were treated with ISO or 5-FU at concentrations of 20-100 μM for 24 h. D) The same cell lines were treated with 27 μM ISO or 5-FU over a time course (6, 12, 18, 24, and 30 h). (*$p < 0.05$, **$p < 0.01$, ***$p < 0.001$ vs. 5-FU) E) Huh-7 cells were stained with Trypan blue and visualized using fluorescence microscopy (scale bar=50 μm). F) Huh-7 cells were stained with Hoechst 33342 and observed by fluorescence microscopy (scale bar=50 μm).

**Figure 2.** Network pharmacology analysis and Molecular Docking analysis of ISO against HCC. A) Chemical structure of ISO. B) Venn diagram of overlapping targets between ISO and HCC. C) PPI network constructed using the MCODE plugin. Nodes with a higher number of connections represent core components. D) KEGG pathway enrichment analysis. E-G) GO enrichment analyses showing biological processes (BP), molecular functions (MF), and cellular components (CC). H) Results of ISO with AKT1, CASP3, and GSK3B.

**Figure 3.** Apoptotic effects of ISO in Huh-7 cells were treated with 27 μM ISO for 0, 3, 6, 12, and 24 h. A) Apoptosis in Huh-7 cells was visualized using Annexin V-FITC/PI staining and fluorescence microscopy (scale bar=50 μm). B) Apoptotic cell percentage was measured via flow cytometry. C) Changes in mitochondrial membrane potential (MMP) were assessed by flow cytometry. D) Apoptotic protein expression levels were analyzed using western blotting. E) Expression of p-ERK, p-JNK, p-p38, and p-STAT3 was evaluated by western blotting. F-H) Huh-7 cells treated with 27 μM ISO and 10 μM MAPK signaling pathway inhibitors for 24 h. Quantitative analysis of Western blotting in F-H results is shown in Supplementary Figure S2. α-tubulin was used as a loading control.

**Figure 4.** Effects of ISO on reactive oxygen species (ROS) accumulation in Huh-7 cells. A) ROS levels were detected by fluorescence microscopy. B) ROS levels in Huh-7 cells treated with 27 μM ISO and/or 10 mM N-acetyl cysteine (NAC) for 24 h. C) Flow cytometry analysis of intracellular ROS levels. D) Apoptosis levels in Huh-7 cells treated with ISO and/or NAC for 24 h, measured by

flow cytometry. E) Western blotting analysis of p-ERK, p-JNK, p-p38, p-STAT3, cle-casp-3, and cle-PARP expression. α-tubulin was used as the internal reference protein.

**Figure 5.** Effects of ISO on cell cycle in Huh-7 cells were treated with 27 μM ISO for 0, 3, 6, 12, and 24 h. A) Fluorescence microscopy analysis of Ki67-stained Huh-7 cells. B) Cell cycle distribution was analyzed via flow cytometry. C) Flow cytometry assessment of cell cycle progression in cells treated with ISO and/or NAC. D) Western blot analysis of G2/M-related proteins. E) ISO and/or NAC treatment for 24 h. F) ISO and/or AKT inhibitor (HY10249) treatment for 24 h. α-tubulin was used as a loading control.

**Figure 6.** Effects of ISO on cell migration in Huh-7 cells were treated with 27 μM ISO for 0, 3, 6, 12, and 24 h. A) Transwell assay for migratory ability (scale bar=100 μm). B) Transwell assay following treatment with ISO and/or NAC for 24 h. (C) Cell migration assay assessing motility (scale bar=100 μm). D) Migration assay after ISO and/or NAC treatment for 24 h. E) Western blotting of migration-associated proteins. F) ISO and/or NAC treatment for 24 h. G) ISO and/or HY10249 treatment for 24 h. α-tubulin served as the internal reference.

**Figure 7.** Schematic diagram of the anticancer mechanisms of ISO in Huh- 7 cells. ISO triggers the accumulation of ROS, which mediates the regulation of multiple signaling pathways. 1. Apoptosis induction: ROS activates MAPK signaling (ERK, JNK, p38), leading to the inhibition of STAT3, downregulation of Bcl- 2, upregulation of Bad, and subsequent activation of the caspase- 3/PARP apoptotic cascade. 2. Cell cycle arrest: ROS suppresses the AKT pathway, resulting in the upregulation of p21 and p27, and the downregulation of CDK1/2 and Cyclin B, thereby arresting the cell cycle. 3. Migration inhibition: ROS inhibits AKT, which inactivates GSK-3β, leading to the downregulation of β-catenin, upregulation of E- cadherin, and downregulation of N- cadherin, ultimately inhibiting cell migration. These effects collectively contribute to the anti- cancer activity of ISO in HCC cells.

Fig. 1 [Download full resolution image]

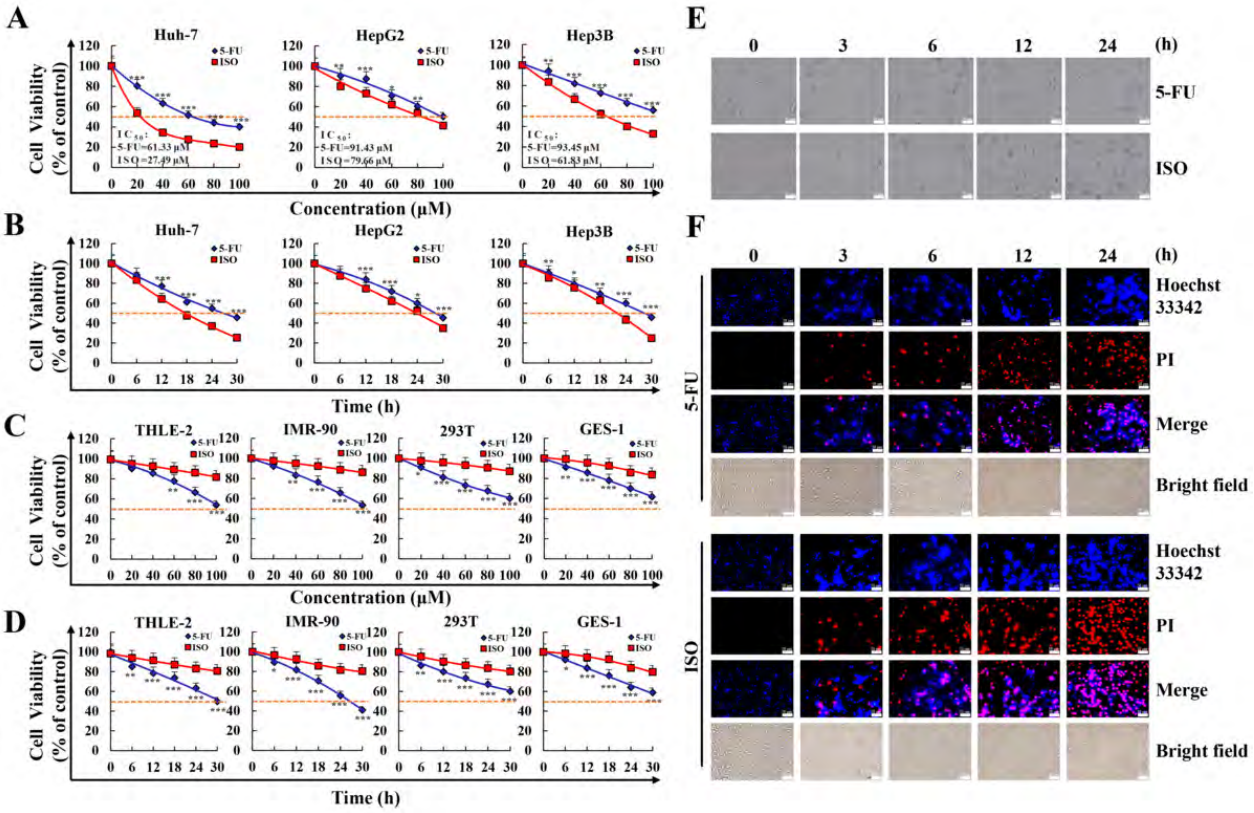

Fig. 2 [Download full resolution image]

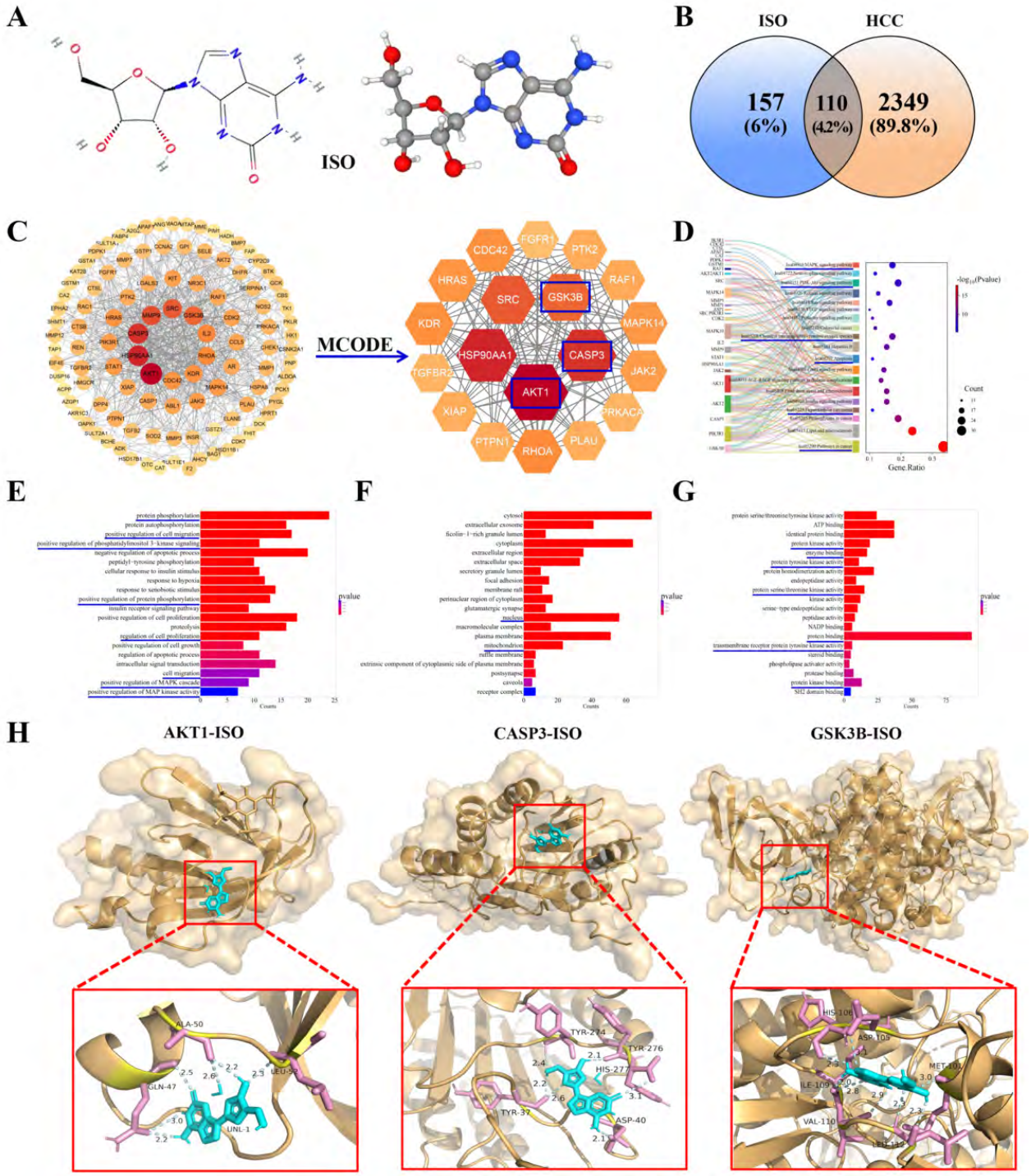

Fig. 3 Download full resolution image

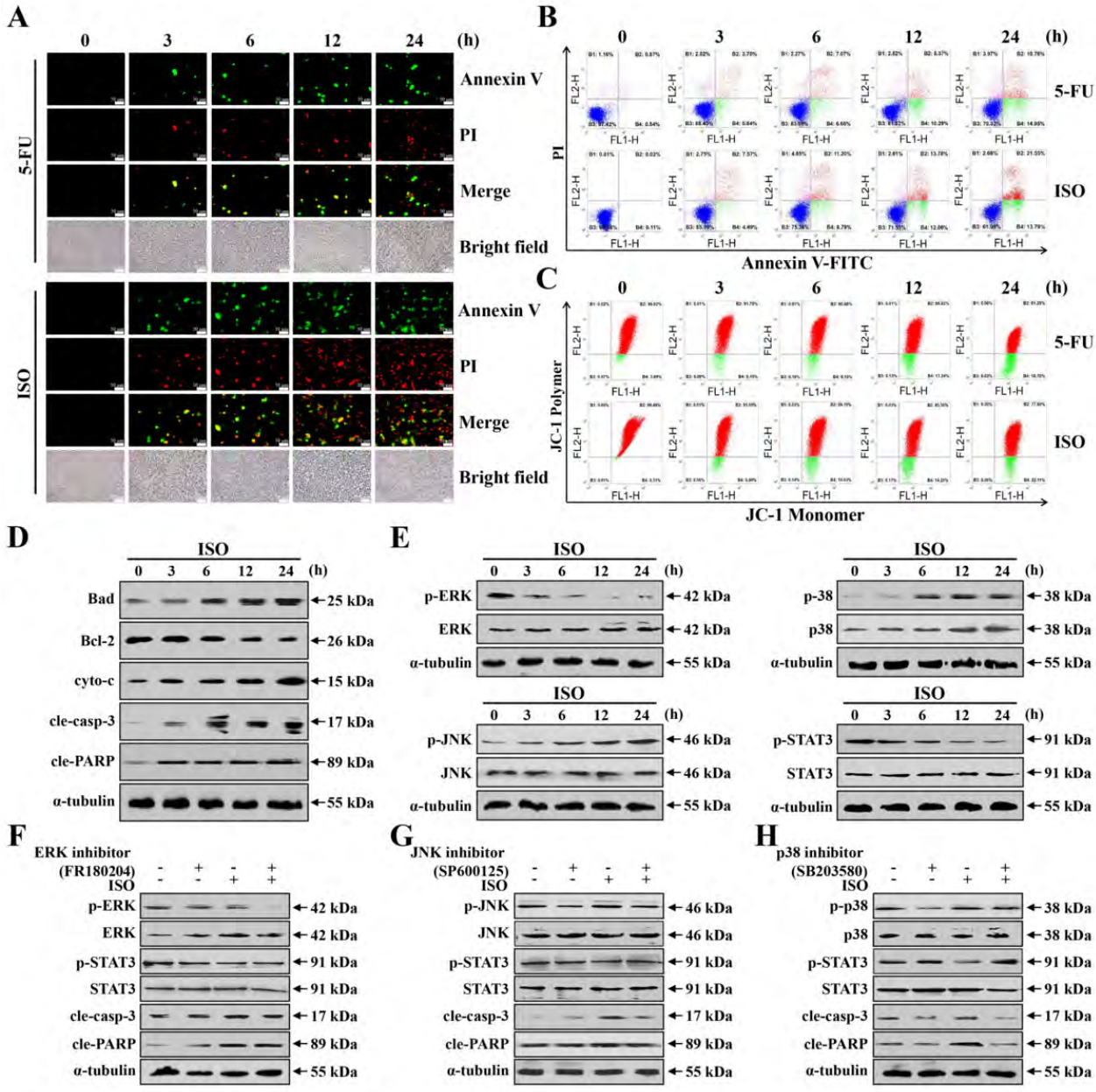

Fig. 4 Download full resolution image

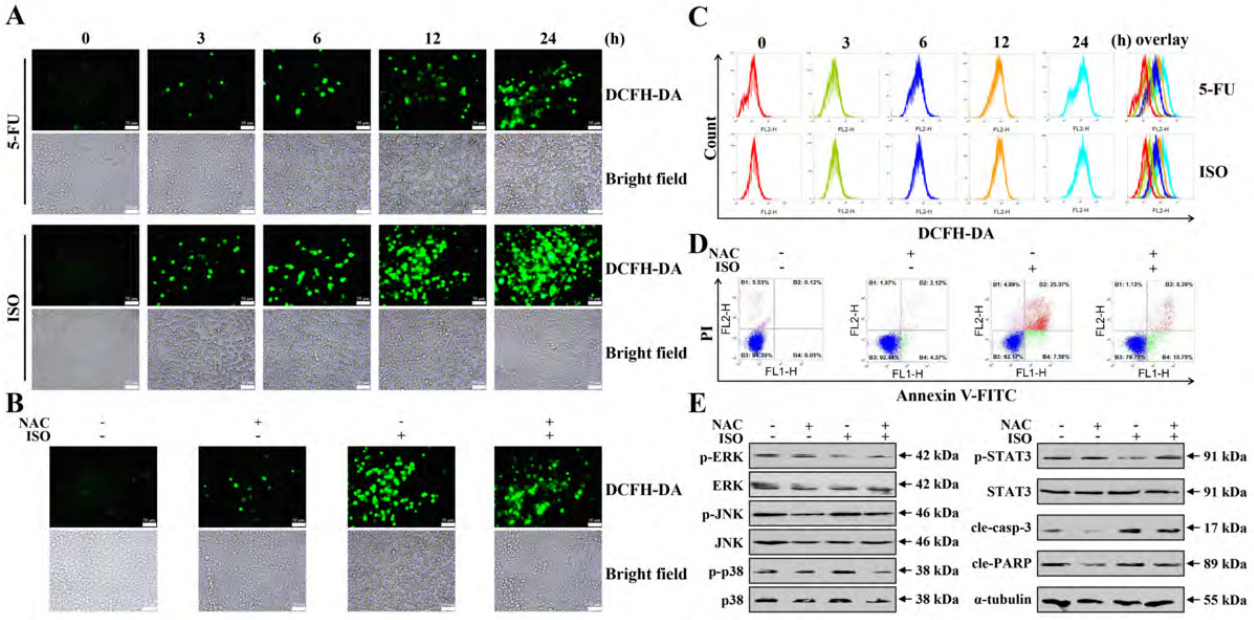

Fig. 5 [Download full resolution image]

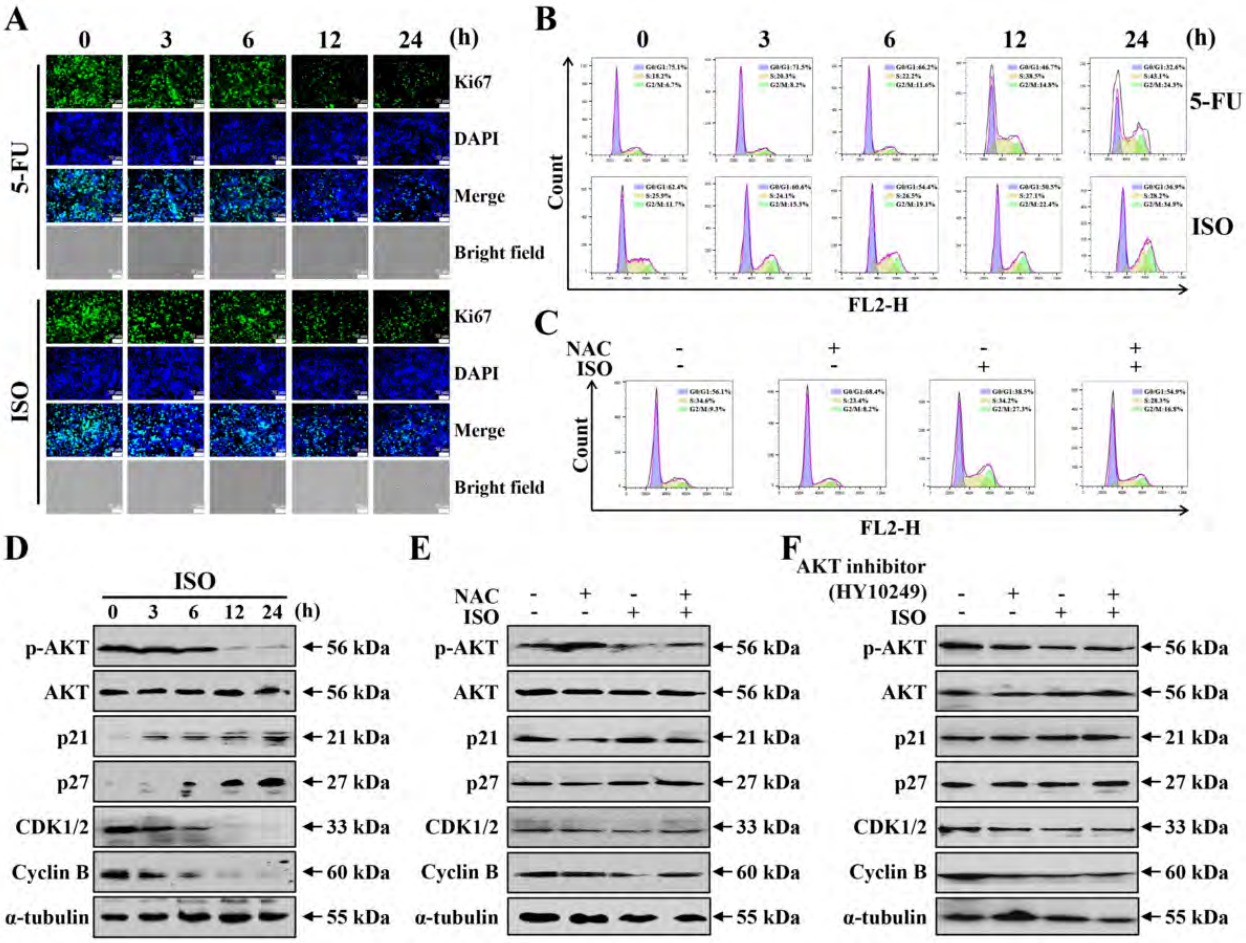

Fig. 6 Download full resolution image

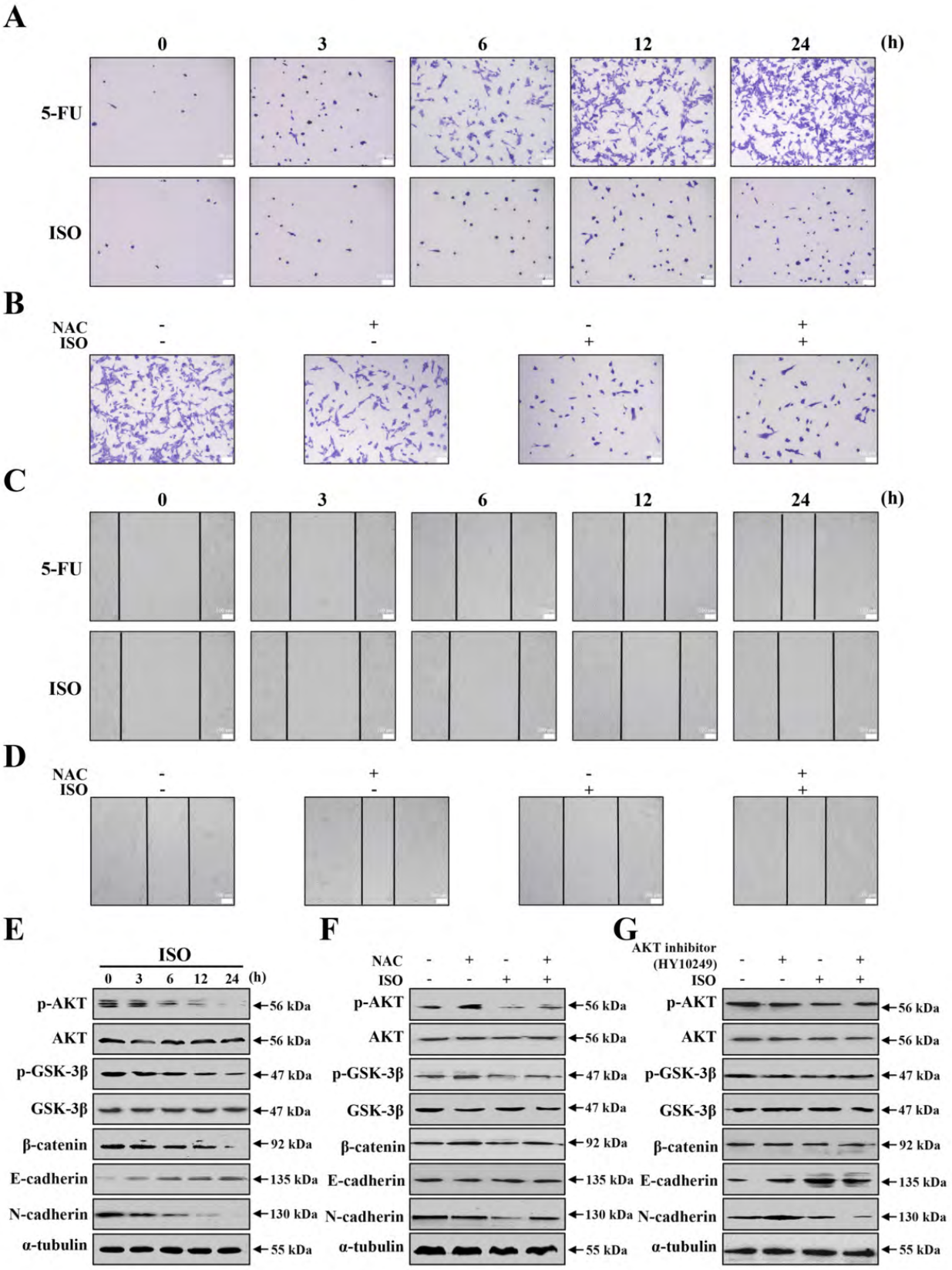

Fig. 7 Download full resolution image